Limnol. Oceanogr., 34(8), 1989, 1510–1523

Modeling in situ phytoplankton absorption from total absorption spectra in productive inland marine waters

Collin S. Roesler and Mary Jane Perry
School of Oceanography, WB-10, University of Washington, Seattle 98195

Kendall L. Carder
Department of Marine Studies, University of South Florida, St. Petersburg 33701

Abstract

Dissolved and suspended materials in the ocean modify the in-water light field by absorbing and scattering photons. Direct measurement of inherent optical properties of individual optical constituents is difficult since the constituents themselves cannot all be separated. A model was developed to resolve in situ phytoplankton absorption from a measured in situ total absorption spectrum which includes water, dissolved organics, particulate detritus, and phytoplankton. The model was tested on a set of absorption spectra obtained from the productive waters around the San Juan Islands, Washington. Results indicate that the model can predict the spectral shape of phytoplankton absorption ($r^2 > 0.9$) and total photon absorption by phytoplankton with <27% error. Total photon absorption can be used to estimate phytoplankton absorption of light energy for improved primary production predictions, given submarine light field measurements or model calculations. Although developed for high chlorophyll waters, the model parameters are easily modified for various Case 1 optical domains.

One current oceanographic goal is to determine global carbon flux in the ocean, which necessitates accurate estimation of primary production. Because photosynthetic rates estimated from ^{14}C uptake and O_2 evolution incubations are fraught with methodological and theoretical problems (Carpenter and Lively 1980; Peterson 1980; Goldman 1988), alternative approaches for determining primary production must be considered. With improved understanding of factors which cause variation in the photosynthetic quantum yield, bio-optical models of photosynthesis based on phytoplankton absorption of light energy and quantum yield can offer a nonincubative, more mechanistic approach to determining primary production (Bannister 1974; Jassby and Platt 1976; Platt and Jassby 1976; Bannister and Weidemann 1984). A problem arises, however, in quantifying in situ phytoplankton absorption. Particulate detritus, including all nonliving cellular material, fecal pellets, heterotrophic bacteria and zooplankton, and dissolved organics (gelbstoff), particularly humic and fulvic acids, are significant absorbers of light. Their presence in natural waters greatly complicates direct measurements of phytoplankton absorption because separation of the absorption spectra of individual components is difficult. Several approaches have recently been developed to obtain estimates of phytoplankton absorption without the effects of detrital or gelbstoff absorption.

The first general approach for estimating phytoplankton absorption is to assume chlorophyll- or accessory pigment-specific absorption coefficients (Bidigare et al. 1989). The second approach is direct measurement of individual cells by microspectrophotometry (Iturriaga et al. 1988; Iturriaga and Siegel 1988) or by flow cytometry (Perry and Porter 1989). The third approach consists of filtering total particulates from a water sample (Yentsch 1962; Kiefer and SooHoo 1982; Mitchell and Kiefer 1984, 1988) and then separating the phytoplankton from the detrital component chemically, statistically, or by modeling (Kishino et al. 1985; Morrow et al. 1989; Cleveland and Perry in prep.). A fourth approach, first introduced

Acknowledgments

This work was supported by NASA grants NAGW 465, NAGW-845, and NAGW-889 and by ONR grants N00014-88-J-1017 and N00014-87-K-0160. We thank M. Kishino, R. F. Davis, and two anonymous reviewers for comments on the manuscript. Special thanks to Dennis Willows for use of laboratory facilities and boat time at the Friday Harbor Laboratories, San Juan Island, Washington. School of Oceanography, University of Washington, contribution 1816.

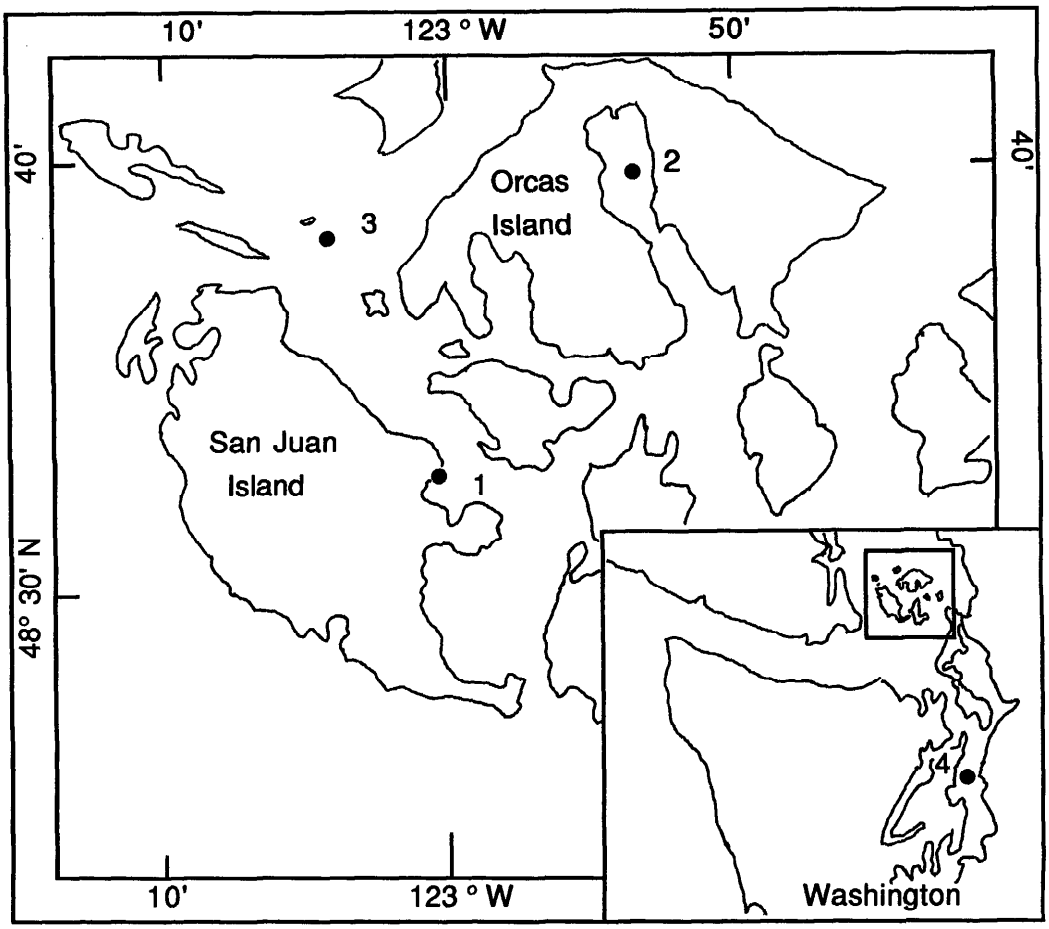

Fig. 1. Study area sites at Friday Harbor dock on San Juan Island (1), East Sound of Orcas Island (2), San Juan Channel (3), and Puget Sound (4).

by Prieur and Sathyendranath (1981) and explored further in this study, is to build upon previous research on the optical properties of water, phytoplankton, detritus, and gelbstoff with the goal of developing a model for determining in situ photon absorption by each of the components from in-water optical measurements.

The major advantage of the model presented here is its ability to separate absorption effects due to individual components while preserving the pigment packaging effects in phytoplankton absorption, which are lost in using specific absorption coefficients for extracted pigments. The model is dependent on simple optical measurements and routine pigment analysis of chlorophyll and pheopigment concentrations. Our component absorption model was developed for the productive and gelbstoff-rich inland marine waters of Washington state where pigment package effects are large. However, by substituting model parameters appropriate for other optical domains, the model can be applied to various oceanic waters, including Case 1 environments.

Methods

A set of 40 particulate and 21 dissolved absorption spectra were obtained from water samples collected with Niskin bottles at three different sites near the San Juan Islands, Washington, in July 1987 (Fig. 1). The Friday Harbor Laboratory dock (FHL, site 1) water is relatively shallow (10 m) and dominated by tidal mixing. East Sound (ES, site

Significant symbols

a_x	Spectrally averaged (400–750 nm) absorption coefficient of component (x) $= \frac{\int a_x(\lambda)\ (m^{-1})\ d\lambda\ (nm)}{750\text{–}400\ nm}$ where x is t (total), w (water), $t - w$, p (total particulate), ϕ (phytoplankton absorption derived from the methanol extraction method of Kishino et al. 1985, including both pigments associated with living phytoplankton and detrital pigments), d ($= p - \phi$), g (gelbstoff), and $d + g$, m^{-1}
$a_x(\lambda)$	Spectral absorption of x, m^{-1}
$a^n_x(\lambda)$	Normalized spectral absorption of x $= \frac{a_x(\lambda)\ (m^{-1})}{a_x\ (m^{-1})}$
$C1_x$	Coefficient of exponential function describing absorption by component d, g, or the sum ($d + g$) (Eq. 6). $C1_x = a_x(400)$, the magnitude of absorption at 400 nm, m^{-1}
$C2_x$	Exponential coefficient which defines spectral shape of the function (*see* $C1_x$ *above*), nm^{-1}
$\phi_{436:676}$	The ratio of $a_\phi(436) : a_\phi(676)$
$\Delta\phi$	The change in $a_\phi(436) : a_\phi(676)$ due to the relative concentrations of pheophytin to chlorophyll (Eq. 15)
λ	Wavelength, nm
$\langle\cdot\rangle$	Symbolizing the ensemble mean of quantity inside angle brackets
$\sigma^2(\cdot)$	Symbolizing ensemble variance of quantity inside parentheses

2) of Orcas Island, a deep fjord (90 m) with a shallow partial sill at the mouth (14 m), exhibits relatively little tidal flushing and can be assumed to be a single water mass. Site 3 in San Juan Channel (SJC) is 120–130 m deep and characterized by strong tidal currents (2 m s^{-1}) and constant flushing through the Strait of Juan de Fuca to the south and the Strait of Georgia to the north. Four additional samples were collected during the following summer and fall (1988) from FHL dock and Puget Sound (site 4). These later samples were used solely to test the model developed with summer 1987 data and were not incorporated in any of the analyses used in model development.

Total particulate absorption spectra [$a_p(\lambda)$] (units given in list of symbols) were measured with an SLM Aminco DW-2C spectrophotometer with the filter pad method of Mitchell and Kiefer (1988) for samples collected on GF/F filters. All particulate absorption spectra were corrected for Mie scattering by subtracting the optical density at 750 nm from the entire spectrum before calculating absorption (*see* Kiefer and SooHoo 1982; Mitchell and Kiefer 1984). Methanol-extractable pigments were removed from the pad with a 10–20-min hot methanol treatment, followed by a 0.2-μm-filtered seawater rinse (modified from Kishino et al. 1985) leaving only a nonmethanol-extractable residue of particulate detritus on the pad. The difference between the particulate and detrital spectra, before and after methanol extraction, is considered to be phytoplankton absorption, although it will tend to overestimate true in vivo phytoplankton absorption because of the inclusion of extractable detrital pigments such as pheophytin and pheophorbide. It is important to note here that in the absence of substantial pheopigment concentrations relative to chlorophyll concentrations (as was the case for the San Juan Island waters), the methanol extraction method provides a good estimate of true in vivo phytoplankton absorption spectra. When the relative pheopigment contribution is substantial, the phytoplankton absorption spectra determined by the Kishino et al. (1985) method must be corrected for pheopigment absorption, as is discussed below.

A 0.2-μm Nuclepore filtrate was used to measure gelbstoff absorption. The spectra were scanned from 400 to 750 nm in 10-cm quartz cuvettes with expanded full scale set equal to 0.01, using freshly collected double glass-distilled water as a reference; optical density was multiplied by 2.3 to convert to an absorption coefficient (m^{-1}). The gelbstoff spectra were low-pass spectrally filtered to remove high-frequency variations associated with the high-sensitivity spectrophotometer setting.

Results

Variance in absorption spectra—Absorption spectra of all samples collected in July 1987 are shown in Fig. 2. The absolute ranges in the magnitude of absorption at 400 nm are 0.03–0.58 m^{-1} for phytoplankton, 0.02–0.19 m^{-1} for detritus, and 0.20–0.39 m^{-1} for gelbstoff. The ensemble mean

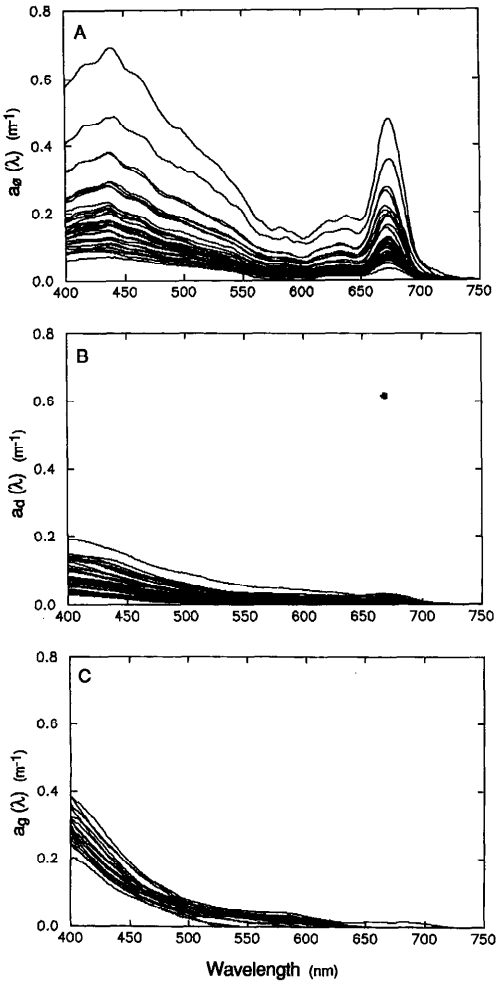

Fig. 2. Absorption spectra collected in July 1987: phytoplankton (A) and detritus (B) derived from the methanol extraction method of Kishino et al. (1985); gelbstoff (C).

absorption spectrum for each component is shown in Fig. 3A together with the clear water absorption curve of Smith and Baker (1981). Blue wavelengths are dominated by absorption due to the particulate and dissolved components while red wavelengths are dominated by water absorption and, to some degree, by the red absorption peak of Chl *a*. The wavelengths of highest transmittance in these waters are 560–570 nm (green–yellow).

In order to model absorption spectra it is necessary to understand and quantify the sources of variance. Absorption spectra exhibit two distinct kinds of variance: variance in magnitude (amplitude) and variance in spectral shape. The sources of magnitude variances are those that contribute to changes in the spectrally averaged component absorption coefficient, a_x, of the sample. Figure 4A shows a hypothetical family of absorption spectra, $a_\phi(\lambda)_i$, for a range of spectrally averaged phytoplankton absorption coefficients, $a_{\phi i}$. Note that the spectral shapes of the curves are identical; thus, for every curve *i*:

$$\frac{a_\phi(\lambda)_i}{a_{\phi i}} = a^n{}_\phi(\lambda), \qquad (1)$$

and $a^n{}_\phi(\lambda)$, the normalized absorption curve, is the same for each of these absorption spectra. The ensemble mean, $\langle a_\phi(\lambda)_i \rangle$, and the ensemble variance, $\sigma^2[a_\phi(\lambda)_i]$, of these spectra are shown in Fig. 4B. The close resemblance between the mean and the variance spectra can be examined mathematically with Eq. 1:

$$\langle a_\phi(\lambda)_i \rangle = \frac{a^n{}_\phi(\lambda)}{N} \times \sum_{i=1}^{N} a_{\phi i} \qquad (2a)$$

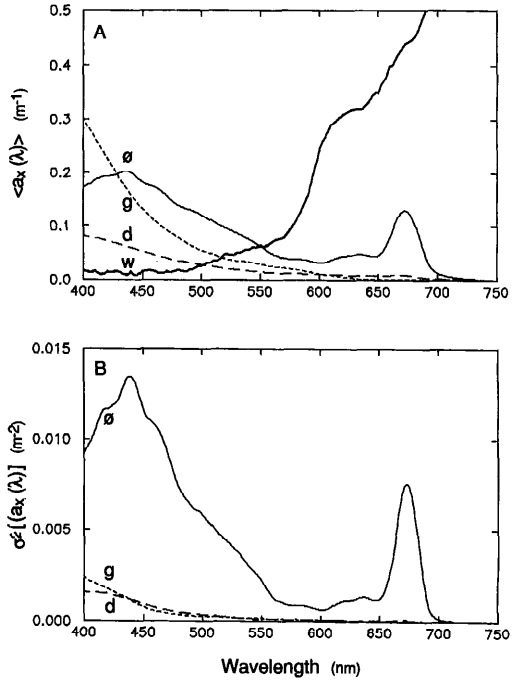

Fig. 3. Ensemble mean (A) and ensemble variance (B) absorption spectra for the phytoplankton (ϕ) detritus (*d*), and gelbstoff (*g*) spectra in Fig. 2. Mean water absorption spectrum (*w*) from Smith and Baker (1981).

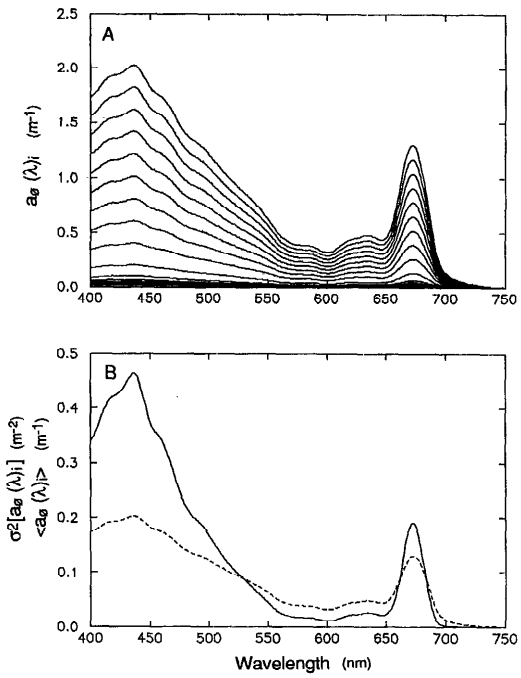

Fig. 4. A. Set of $i = 1, 19$ phytoplankton absorption spectra, with identical spectral shape defined by $a^n_\phi(\lambda)$, with varying spectrally averaged absorption coefficients, $a_{\phi i}$ (m^{-1}), given by

$$a_\phi(\lambda)_i = a_{\phi i} \times a^n_\phi(\lambda).$$

B. The ensemble mean (dotted) and variance in magnitude (solid) of the set of 19 spectra in panel A.

and

$$\sigma^2[a_\phi(\lambda)_i] = \frac{a^n_\phi(\lambda)^2}{N} \times \sum_{i=1}^{N} (a_{\phi i} - \langle a_{\phi i}\rangle)^2 \quad (2b)$$

where $\langle a_{\phi i}\rangle$ is the ensemble mean of the spectrally averaged absorption coefficients for the set of $N = 19$ phytoplankton absorption spectra. The squared normalized absorption term in Eq. 2b accounts for the peakedness of the variance spectrum relative to the mean spectrum.

The variance in the spectral shape of the absorption curves is a consequence of variations in the contribution of various pigment absorption bands, primarily due to changes in the composition of accessory pigments. Pigment packaging can be a more subtle source of spectral variance by flattening the absorption peak for large absorbing cells (Morel and Bricaud 1981; Bricaud et al. 1988; Kirk 1983). The variance due solely to changes in spectral shape is examined in Fig. 5A for 14 different species of phytoplankton. Each spectrum $[a_\phi(\lambda)_k$, where $k = 1, 14]$ has been normalized to its respective spectrally averaged absorption coefficient ($a_{\phi k}$) to remove concentration and major packaging effects:

$$a^n_\phi(\lambda)_k = \frac{a_\phi(\lambda)_k\ (m^{-1})}{a_{\phi k}\ (m^{-1})} \quad (3)$$

where the superscript n indicates normalized absorption and, unlike the previous hypothetical case, the set of 14 normalized absorption spectra are not identical in shape.

The ensemble mean, $\langle a^n_\phi(\lambda)_k\rangle$, and ensemble variance, $\sigma^2[a^n_\phi(\lambda)_k]$, of these spectra are shown in Fig. 5B. There is no simple relation between the mean and the spectral variance, nor do the two spectra resemble each other. The peaks in spectral variance are associated with differences in pigmentation, such as Chl *b* and *c* and photosynthetic carotenoids. In a seawater sample, fluctuations in the proportions of humic and fulvic acids directly influence the spectral shape of gelbstoff absorption spectra (Carder et al. 1989) in an analogous manner. It can be expected that compositional changes in the particulate detritus component will likewise cause spectral variations in detrital absorption.

Variance in field absorption spectra—The ensemble variance curve calculated for the raw absorption spectra in Fig. 2 combines the effects of variation in magnitude and spectral shape (Fig. 3B) but, by resembling the ensemble mean curve, behaves in the manner predicted for magnitude variations. This indicates that variations in concentration of pigments, humic and fulvic acids, and detrital composition and pigment packaging effects are dominating the component ensemble variance signals. At 400 nm, the ensemble variance is approximately equivalent to standard deviation values of 51, 53, and 17% of the mean value of phytoplankton, detrital, and gelbstoff absorption.

However, normalizing the raw component absorption spectra in Fig. 2 to their respective spectrally averaged absorption

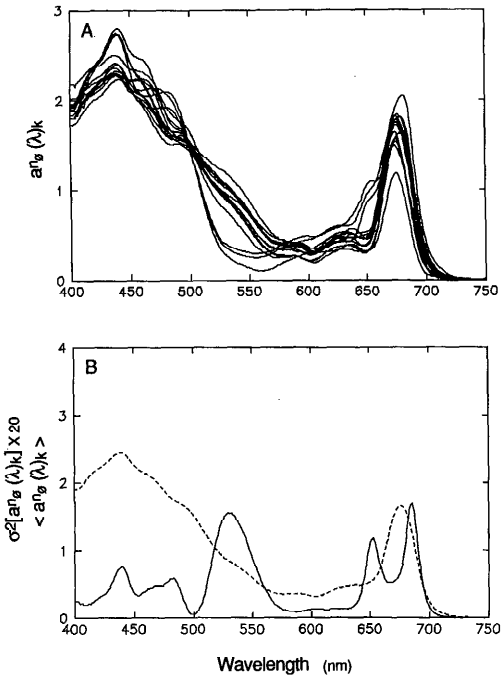

Fig. 5. A. Set of measured absorption spectra from 14 clones of phytoplankton species representing diverse taxonomic groups: dinoflagellates (*Amphidinium carterae, Glenodinium* sp. UTEX 1652, *Peridinium triquetrum*), prymnesiophytes (*Isochrysis galbana, Pavlova lutheri*), diatoms (*Chaeotoceros gracilis, Cylindrotheca fusiformis, Nitzschia closterium, Phaeodactylum tricornium, Skeletonema costatum, Thalassiosira weisflogii*), prasinophyte (*Pyramimona parkerae*), and chlorophytes (*Dunaliella euchlora, Nannochloris* sp.) (from Perry and Porter 1989). Each spectrum is normalized to its respective spectrally averaged absorption coefficient to remove the effects of concentration and major packaging. The $k = 1, 14$ normalized absorption spectra are given by

$$a^n_\phi(\lambda)_k = \frac{a_\phi(\lambda)_k}{a_{\phi k}}.$$

B. The ensemble mean (dotted) and variance in spectral shape (solid) of the set of 14 spectra in panel A.

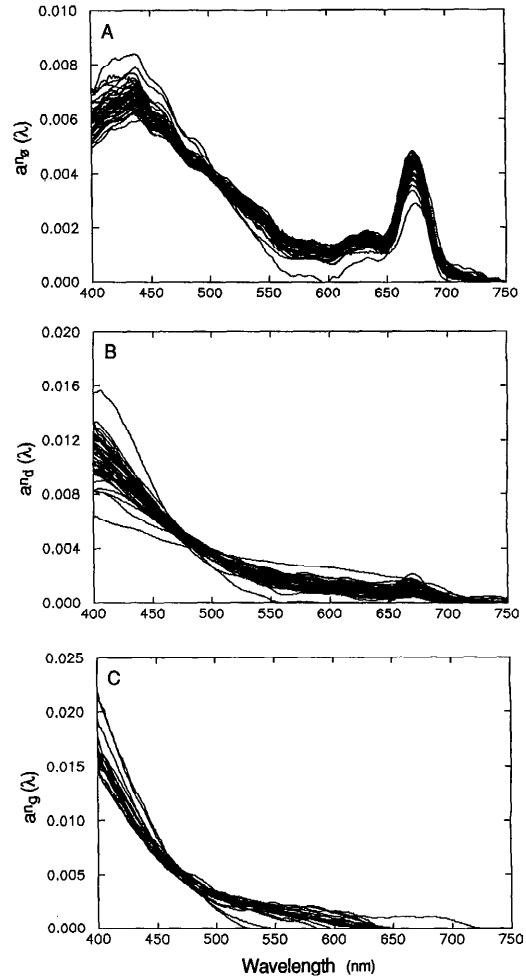

Fig. 6. Absorption spectra in Fig. 2 normalized to their respective spectrally averaged absorption coefficients to emphasize variations in spectral shape: phytoplankton (A), detritus (B), and gelbstoff (C).

coefficients (as in Eq. 3) removes the effect of concentration (Fig. 6) and allows computation of ensemble variance due solely to spectral shape. The ensemble variance in the spectral shape of phytoplankton absorption (Fig. 7A) no longer covaries with the ensemble mean curve. The greatest variance in spectral shape coincides with the blue and red absorption peaks of the chlorophylls and the accessory pigment absorption peaks. The increased variance in the blue region compared with that generated by the absorption spectra of the cultured phytoplankton species is due to inclusion of the pheopigments in these phytoplankton absorption spectra. The variance in spectral shape of both gelbstoff and detritus (Fig. 7B, C) is greatest in the far blue region (400–425 nm).

The variance in spectral shape is approximately equivalent to standard deviations of 9, 20, and 11% of the mean values of phytoplankton, detritus, and gelbstoff at 400 nm. These values relative to the variations in the raw curves (Fig. 3B) indicate that the

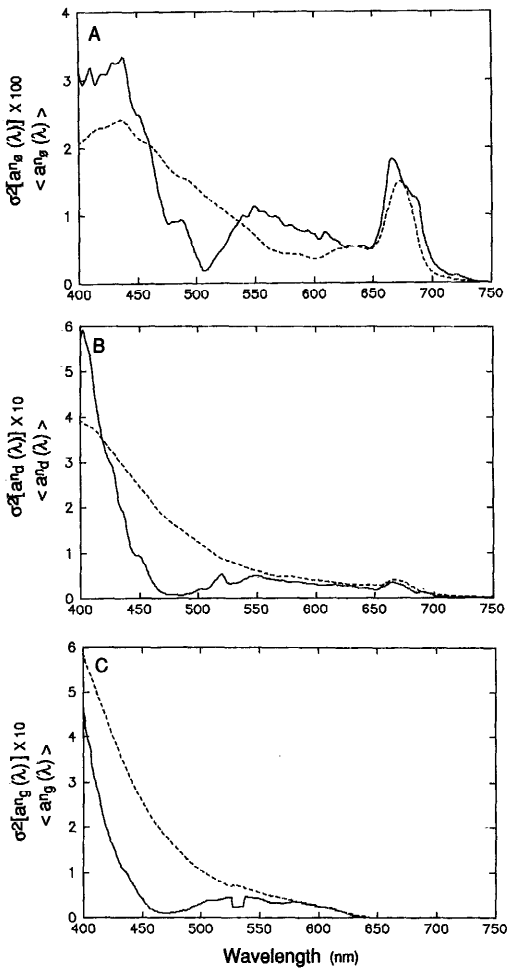

Fig. 7. Ensemble mean (dashed) and variance (solid) for the normalized absorption spectra in Fig. 6. The ensemble variance curves were multiplied by the factors indicated and are equivalent to standard deviations of 9% of the mean value at 400 nm for phytoplankton, 20% for detritus, and 11% for gelbstoff.

variability in phytoplankton absorption for these waters is dominated by fluctuations in phytoplankton concentration, with a small contribution to variance by changes in pigment composition; that the variability in detrital absorption is due to both concentration and compositional changes; and that the variability in gelbstoff absorption is low and is almost equally regulated by concentration and by compositional changes.

Discussion

Model development—Phytoplankton absorption spectra are complex with potentially large variations in both magnitude and spectral shape; the consequence of this variability is that direct modeling of phytoplankton absorption from total in-water absorption measurements will be difficult. On the other hand, the magnitude and spectral variability exhibited by the detrital and gelbstoff components is much lower and is confined to the far blue region of the spectrum. The implication of their relatively low variability over the remaining spectral range (425–750 nm) is that their absorption spectra can be modeled with reasonable accuracy. Total absorption $[a_t(\lambda)]$ can be represented as

$$a_t(\lambda) = a_w(\lambda) + a_\phi(\lambda) + a_d(\lambda) + a_g(\lambda). \quad (4)$$

Recent advances in the technology of optical instrumentation may soon allow the measurement of total in-water absorption spectra. These include the flow-through photoacoustic method for measuring profiles of total absorption (Trees and Voss 1988) and an in-water absorption meter (Zaneveld et al. 1988). Total absorption spectra can also be estimated from measurements of spectral upwelling and downwelling irradiance and the solar zenith angle (Morel and Prieur 1975) and from measurements of remote-sensing reflectance corrected for scattering (Carder et al. 1986). Absorption due to water is generally well defined (Morel 1974; Smith and Baker 1981) and can be specified and hence removed from the total absorption spectrum. If we allow $a_{t-w}(\lambda)$ to represent the measured total absorption spectrum with water absorption removed, the phytoplankton absorption spectrum can be determined by

$$a_\phi(\lambda) = a_{t-w}(\lambda) - [a_d(\lambda) + a_g(\lambda)]. \quad (5)$$

Previous studies have successfully modeled gelbstoff absorption using exponential functions (e.g. Jerlov 1968; Morel and Prieur 1976; Bricaud et al. 1981; Okami et al. 1982; Carder et al. 1989). The general shape of the nonextractable detrital absorption spectra suggests that it can be similarly modeled and perhaps combined with gelbstoff absorption. The general exponential function

$$a_x(\lambda) = C1_x \times \exp[-C2_x \times (\lambda - 400)] \quad (6)$$

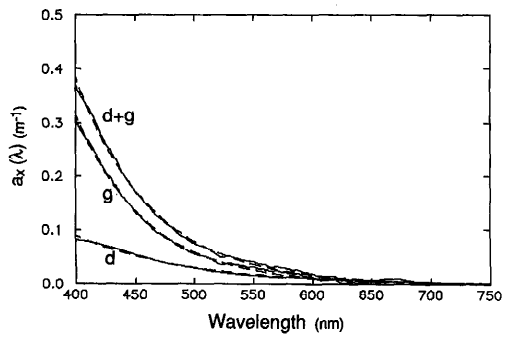

Fig. 8. Ensemble mean (solid) and exponentially modeled (dashed) absorption spectra of detritus ($x = d$), gelbstoff ($x = g$), and the sum ($x = d + g$), where the model is defined by Eq. 6.

can be used to describe the absorption spectrum.

The ensemble mean absorption spectra for the original data [$a_d(\lambda)$, $a_g(\lambda)$, and $a_{d+g}(\lambda)$] and the ensemble mean spectra modeled according to Eq. 6 are shown in Fig. 8. Values of $C1_x$ for detritus, gelbstoff, and their sum are 0.09, 0.32, and 0.38 for the July 1987 data; values of $C2_x$, which define the spectral shape of the curves, are 0.011, 0.017, and 0.016. The mean and standard deviations for $C2_d$ and $C2_g$ determined for our data were almost identical to the literature means and standard deviations reported for various sites and water types, suggesting that the range of values we obtained is representative for many oceanic sites (Table 1).

The success of modeling the combined detrital and gelbstoff absorption with a single exponential function allows Eq. 5 to be expressed as

$$a_\phi(\lambda) = a_{t-w}(\lambda) - C1_{d+g} \times \exp[-C2_{d+g} \times (\lambda - 400)]. \quad (7)$$

The value of the $C1_{d+g}$ coefficient is linearly dependent on the values of $C1_d$ and $C1_g$ and is determined by

$$C1_{d+g} = C1_d + C1_g. \quad (8)$$

Table 1. Ranges for the exponential coefficient, $C2_x$, for gelbstoff and detritus for Eq. 6. Where coefficients were not listed, values were approximated from published spectra using an exponential model.

Reference	Site	Avg $C2_x$ (nm^{-1})
Gelbstoff		
Kalle 1966	Baltic, North Sea	0.018
Jerlov 1968		0.015
Kirk 1976	Lakes, coast	0.015
Lundgren 1976	Baltic	0.014
Kopelevich and Burenkov 1977	Indo-Pacific	0.017
Bricaud et al. 1981	Baltic	0.018
	Mauritania	0.015
	Gulf of Guinea	0.014
	Mediterranean	0.014
Okami et al. 1982	East Pacific	0.017
Kishino et al. 1984	Lake Kizaki	0.016
	Nabeta Bay	0.015
	East Pacific	0.014
Carder and Steward 1985	Gulf of Mexico	0.014
Davies-Colley and Vant 1987	Lakes	0.019
Maske and Haardt 1987	Kiel Harbor	0.016
Published mean ± SD		0.016±0.002
This study mean ± SD	San Juan Islands	0.017±0.003
Carder et al. 1989	Marine humic acid	0.011
	Marine fulvic acid	0.018
Detritus		
Kishino et al. 1986	NW Pacific Ocean	0.006
Maske and Haardt 1987	Kiel Harbor	0.014
Iturriaga and Siegel 1988	Sargasso Sea	0.011
Cleveland and Perry in prep.	Sargasso Sea	0.013
Morrow et al. 1989	Sargasso Sea	0.009
Published mean ± SD		0.011±0.002
This study mean ± SD	San Juan Islands	0.011±0.002

However, a linear combination of the absorption spectra of the two components results in a nonlinear expression for the exponential coefficient, $C2$, of the detritus plus gelbstoff model:

$$C2_{d+g} = \frac{1}{\lambda - 400}\{\ln(C1_d + C1_g) - \ln[a_d(\lambda) + a_g(\lambda)]\}. \quad (9)$$

As discussed in the previous section, variability due to changes in magnitude is determined by fluctuations in the concentrations of the absorbing substances—detritus and gelbstoff. This source of variability will be manifested as variability in the $C1_{d+g}$ coefficient. Spectral variability, on the other hand, is determined by the relative concentrations of the two components as well as the variability due to compositional changes within each component. This source of variability is manifested as variability in the $C2_{d+g}$ coefficient (as exhibited by the range of values for each component in Table 1). It is important to note that the value of $C2_{d+g}$ is always constrained by the specific values of $C2_d$ and $C2_g$ for the sample; the value for the sum cannot lie outside the range of the individual values; rather, it will be closer to the component of greatest concentration. Thus, for waters dominated by gelbstoff absorption (such as the San Juan Island waters) $C2_{d+g}$ will be closer to values of 0.016, while for waters dominated by detrital absorption (such as the oligotrophic open ocean; cf. Højerslev 1980) the value of $C2_{d+g}$ will be closer to 0.011. Values for coastal regions might be expected to be intermediate between the two extremes.

No correlation between $C2_d$ and $C2_g$ was found for this data set (Spearman's Rank correlation, $P > 0.2$) and thus no further constraints on $C2_{d+g}$ could be established. To estimate the maximum error in $a_{d+g}(\lambda)$ that would result by incorrectly estimating $C2_{d+g}$, we computed the percent difference in the spectrally averaged absorption coefficient a_{d+g} from two extreme water conditions by setting $C1_{d+g}$ equal to 1.0 and allowing $C2_{d+g}$ to equal either a pure detritus value of $C2$ (more typical of oceanic regions) or a pure gelbstoff value of $C2$ (more representative of estuarine regions). The worst case scenario results from using the extreme literature values of $C2_d$ and $C2_g$ for the $C2_{d+g}$ coefficient for the two water conditions (0.006 and 0.019; Table 1). The spectrally averaged absorption coefficient from the two spectra differ by a factor of $< \pm 1.5$ from their ensemble mean value. A more realistic error would result from selecting coefficient values that are ~1 SD too high or low [$\sigma = 0.002$ (nm^{-1}), Table 1] from the mean value, resulting in an error estimate of $\pm 7\%$ from the mean spectrally averaged absorption coefficient for detritus plus gelbstoff.

The magnitude of the 400-nm absorption value ($C1_{d+g}$) will be highly variable spatially and temporally. However, with the exponential model, if a value for $a_{d+g}(\lambda)$ can be uniquely determined at any one wavelength (λ_o), the value of $C1_{d+g}$ can be uniquely determined by inverting Eq. 6 and estimating $C2_{d+g}$:

$$C1_{d+g} = a_{d+g}(400) = a_{d+g}(\lambda_o) \times \exp[C2_{d+g} \times (\lambda_o - 400)]. \quad (10)$$

Hence, the entire detritus plus gelbstoff spectrum can be described by

$$a_{d+g}(\lambda) = \{a_{d+g}(\lambda_o) \times \exp[C2_{d+g} \times (\lambda_o - 400)]\} \times \exp[-C2_{d+g} \times (\lambda - 400)] \quad (11)$$

with $a_{d+g}(\lambda_o)$ being the only unknown quantity. The key to determining $C1_{d+g}$ is to identify some wavelength (λ_o) at which detritus plus gelbstoff absorption can be uniquely determined.

One inherent assumption of the Kishino et al. (1985) methanol extraction method is that all pigment absorption at 676 nm is included with the phytoplankton absorption; hence, the total absorption at 676 nm (corrected for water absorption) is due primarily to the extracted-phytoplankton absorption (chlorophylls and pheopigments) with only a minor contribution by the tail end of the exponential curve for detrital and gelbstoff absorption. The detrital and gelb-

stoff spectra in Fig. 2B and C confirm that absorption by either component is minor at 676 nm (always <10% and generally closer to 1%, although incomplete methanol extraction of pigments may account for the larger percentages). If the assumption is made that $a_{d+g}(676)$ is negligible in comparison to $a_\phi(676)$ [i.e. $a_\phi(676) = a_{t-w}(676)$], then the ratio of total absorption at the blue and red phytoplankton absorption peaks,

$$\frac{a_{t-w}(436)}{a_{t-w}(676)} = \frac{a_\phi(436) + a_{d+g}(436)}{a_\phi(676) + a_{d+g}(676)}, \quad (12)$$

can be rearranged to yield

$$a_{d+g}(436) = a_{t-w}(436) - a_{t-w}(676) \times \phi_{436:676} \quad (13)$$

where $\phi_{436:676}$ is the blue-to-red absorption peak ratio for phytoplankton. Thus, if $\phi_{436:676}$ is known, $a_{d+g}(436)$ can be uniquely determined and the entire detritus plus gelbstoff absorption spectrum can be modeled from Eq. 11 with $\lambda_o = 436$ nm. The phytoplankton absorption spectrum can be subsequently modeled as

$$a_\phi(\lambda) = a_{t-w}(\lambda) - a_{d+g}(\lambda). \quad (14)$$

Estimating model parameters: $\phi_{436:676}$ and $C2_{(d+g)}$—The appropriate selection of $\phi_{436:676}$, which can change with species, light history, nutrients, pigment composition, and package effects (cf. Sathyendranath et al. 1987; Bricaud et al. 1988), is critical to the model. Carotenoids, xanthophylls, and Chl *c* contribute to absorption only at 436 nm and not at 676 nm, thus increasing the value of $\phi_{436:676}$ as a linear function of their concentration. Chl *b* contributes only minor absorption at 676 nm relative to 436 nm. Growth irradiance may alter $\phi_{436:676}$ by stimulating increased synthesis of photoprotective pigments at higher irradiances (Fig. 9A). A similar trend of increased $\phi_{436:676}$ at higher irradiances was also observed in field samples as a function of in situ irradiance (Fig. 9B).

The red peak (676 nm) of the Kishino et al. (1985) phytoplankton absorption is primarily a function of absorption by Chl *a* and pheopigments. Extracted pheophytin *a* has a blue-to-red peak ratio approaching 2.1 (Hendry et al. 1987); its blue and red absorption peaks are shifted relative to those of Chl *a* (~20 nm to the ultraviolet and 5 nm to the infrared; Vernet and Lorenzen 1987). Assuming that the relative offset in absorption peaks between pheophytin *a* and Chl *a* in acetone hold qualitatively for in vivo pigments, it can be concluded that pheophytin *a* contributes relatively more absorption to the 676-nm peak than to the 436-nm peak (Fig. 10A), thus effectively reducing the value of $\phi_{436:676}$ by a quantity $\Delta\phi$ as the ratio of pheophytin *a* to Chl *a*, [Pheo]:[Chl], increases (Fig. 10B). A nonlinear fit to the points in Fig. 10B ($r^2 = 0.99$) allows the dependence of $\phi_{436:676}$ on the ratio of pheophytin *a* to Chl *a* to be quantified by

$$\Delta\phi = 0.6 \times \left\{1 - \exp\left(-0.7 \times \frac{[\text{Pheo}]}{[\text{Chl}]}\right)\right\} \quad (15)$$

which approaches zero when Chl *a* concen-

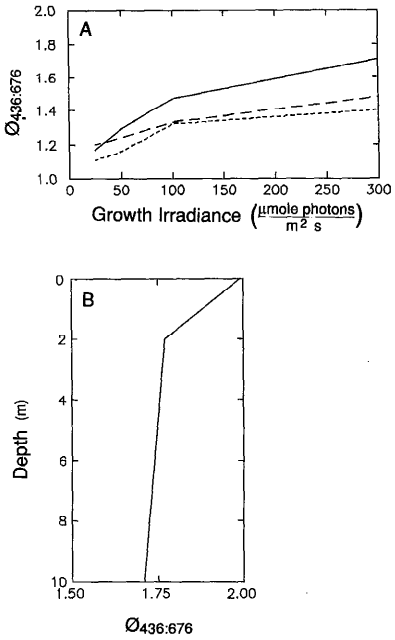

Fig. 9. A. Blue-to-red phytoplankton absorption peak as a function of growth irradiance for three species of cultured phytoplankton: *Amphidinium carterae* (dinoflagellate containing Chl *a* and *c*2, solid), *Thalassiosira weisflogii* (centric diatom containing Chl *a*, *c*1, and *c*2, dashed), and *Dunaliella euchlora* (chlorophyte containing Chl *a* and *b*, dotted). (Data from Perry and Porter 1989.) B. Depth distribution of $\phi_{436:676}$, from FHL dock samples 29 July 1987, 1400 hours.

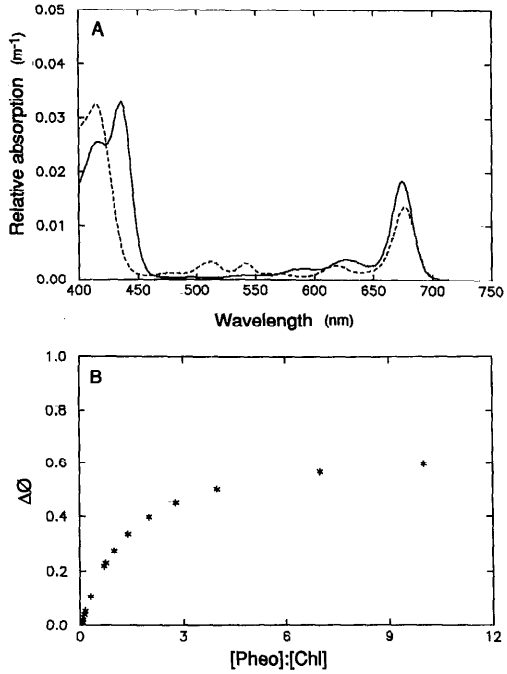

Fig. 10. A. In vivo Chl *a* (solid) and pheophytin (dashed) absorption spectra (modified from acetone extractions). Units are in relative absorption. B. The change in the blue-to-red (436:676 nm) absorption peak ratio, $\Delta\phi$, due to varying the extracted pheophytin-to-Chl *a* ratio. Calculated from varying relative magnitudes of the Chl *a* and pheophytin spectra in panel A. Nonlinear regression onto the points is given by Eq. 15 with $r^2 = 0.99$.

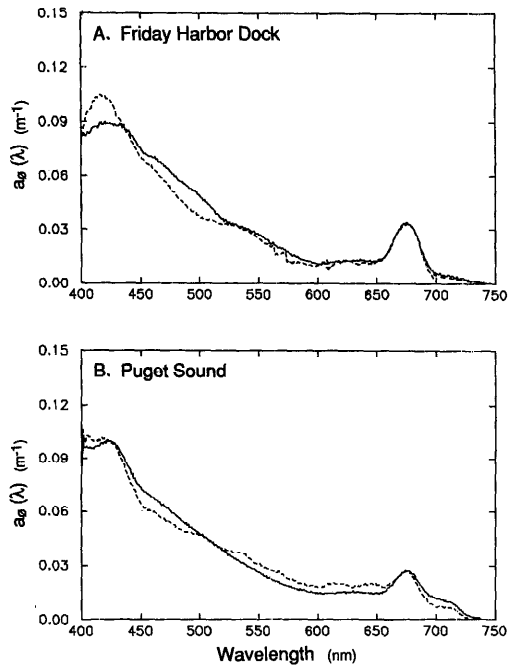

Fig. 11. Two examples of measured (solid) and modeled (dashed) phytoplankton absorption spectra from the 1988 samples.

trations are relatively much greater than pheopigment concentrations and approaches 0.5 when pheopigment concentrations are relatively large.

For this study, values for $\phi_{436:676}$ were selected based on an average value typical of large, coastal diatoms and dinoflagellates (1.8)—the dominant phytoplankton groups found in these waters—scaled by $\Delta\phi$ according to the relative concentrations of pheopigment and chlorophyll in each sample, resulting in

$$\phi_{436:676} = 1.8 - \Delta\phi. \qquad (16)$$

An average value of $\phi_{436:676}$ can be assigned regionally, based on the presence or absence of cyanobacteria, prochlorophytes, and prasinophytes (Morrow et al. 1989; Cleveland and Perry in prep.), while $\Delta\phi$ requires only routine measurements of Chl *a* and pheopigment.

Selection of the most appropriate value for $C2_{d+g}$ can be based on historical or simultaneous observations of the specific site. As discussed in the previous section, predicting the ratio between detritus and gelbstoff narrows the range of possible values of $C2_{d+g}$ considerably. Average values of $C2_{d+g}$ range between 0.011 (detrital and humic acid dominance) and 0.016 (fulvic acid dominance). For evaluation of the model, a value of 0.015 for $C2_{d+g}$ was selected from the literature mean values of $C2_d$ (0.011) and $C2_g$ (0.016) based on a detritus-to-gelbstoff ratio of 1:4, which is appropriate for the waters of the San Juan Islands.

Model evaluation and correction—Two examples of measured and modeled phytoplankton absorption spectra are shown in Fig. 11. A statistical indication of the prediction of spectral shape is given by the correlation values (Table 2). In 22 of the 25 cases the correlation between modeled and measured spectral shape is >0.96. The largest error in estimating the spectrally averaged phytoplankton absorption coefficient

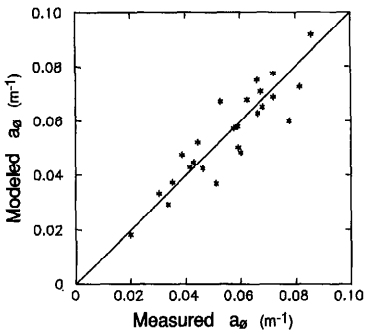

Fig. 12. Modeled vs. measured spectrally averaged phytoplankton absorption coefficient. Solid line represents one-to-one correlation. The regressed slope is not significantly different from 1.0 at the 99% C.L. The mean relative difference between the measured and modeled data is 10.3%.

(Fig. 12) is 27.6%, although 19 of the 25 predictions exhibit <15% error (Table 2). Thus, it appears that the model can accurately predict both the spectral shape and magnitude of a phytoplankton spectrum, including the effects of pigment packaging, based on the Kishino et al. (1985) methanol extraction method.

Estimates of the total number of available photons absorbed by phytoplankton are required for bio-optical production models because photosynthesis is a quantum event. Total photon absorption by phytoplankton is dependent not only on the shape of the phytoplankton absorption spectrum, but also on the magnitude of the integrated absorption coefficient. The major drawback of the methanol extraction method for determining phytoplankton spectral absorption coefficients is that it systematically overestimates the photons absorbed for photosynthesis by including absorption by the nonphotosynthetic carotenoids and detrital pigments. These pigments do not contribute energy to photosynthesis and should more appropriately be included in the detrital component, although, the effects of nonphotosynthetic carotenoids can be compensated for in photosynthesis models by selection of a reduced photosynthetic quantum efficiency coefficient. Detrital pigment absorption can be removed from a Kishino et al. (1985) phytoplankton spectrum by subtracting a pheopigment absorption spectrum computed from the pheophytin spectrum in Fig. 10A scaled into absolute units at 676 nm according to the relative concentration of pheopigment to Chl *a* in the sample. An example of a corrected and uncorrected phytoplankton absorption spectrum is shown in Fig. 13. It should be noted that whatever packaging effects operate on in vivo pheopigment absorption are lost in this first-order method of correction.

The significance of the phytoplankton absorption model presented here is that it is

Table 2. Results of the comparison between model estimated and measured phytoplankton absorption spectra, $a_\phi(\lambda)$ (m^{-1}), from July 1987 and August 1988. Sample specific $\phi_{436:676}$ values were computed from Eq. 16 based on measured pheopigment-to-Chl *a* ratios. Spectral correlation, ρ, measures the statistical accuracy of the model-predicted spectral shape of the phytoplankton absorption spectrum. Correlation values of 0.99+ indicate >0.995 correlation. Percent error indicates the error in model-estimated vs. measured spectrally averaged phytoplankton absorption coefficients, a_ϕ (m^{-1}).

Depth	$\phi_{436:676}$	ρ	% error
Friday Harbor dock			
0*	1.70	0.99	+3.3
0	1.67	0.96	−27.2
2	1.73	0.99	+4.4
5	1.70	0.99	−19.5
5	1.75	0.98	+17.5
5	1.71	0.96	+3.1
5	1.74	0.99	−4.1
5	1.69	0.97	+27.6
10	1.73	0.96	+22.7
East Sound			
0	1.80	0.99+	−14.8
2	1.80	0.99	−22.5
4	1.80	0.97	−10.8
10	1.79	0.99	−1.3
16	1.79	0.93	+10.0
San Juan Channel			
0	1.80	0.99+	+6.7
0	1.72	0.99+	0.0
4	1.80	0.99+	+5.2
4	1.71	0.99+	−4.3
9	1.72	0.99	+7.6
10	1.80	0.99	+13.9
19	1.80	0.99	−5.2
26	1.67	0.99+	+8.9
Puget Sound			
0*	1.50	0.95	+8.0
10*	1.50	0.99	+0.3
50*	1.35	0.93	−8.4

* 1988 sample.

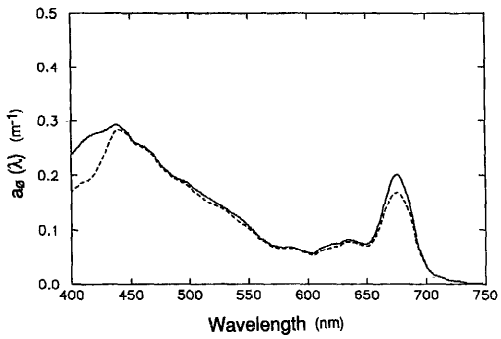

Fig. 13. Measured phytoplankton absorption spectrum (solid) corrected for pheopigment absorption dashed) based on the pheophytin *a* absorption curve n Fig. 10A. The curve in Fig. 10A is scaled to true)heophytin *a* absorption units (m^{-1}) by partitioning $a_\phi(676)$ into contributions by Chl *a* and pheophytin *a*. True pheophytin *a* absorbtion at 676 nm equals $a_\phi(676) \times \{0.58[\text{Pheo}]/([\text{Chl}] + 0.58[\text{Pheo}])\}$, where 0.58 represents the reduction in the specific absorption coefficients of pheophytin *a* relative to Chl *a* (Lorenzen and Jeffrey 1980).

ndependent of chlorophyll-specific absorption coefficients and assumptions about the nagnitude or shape of the phytoplankton ıbsorption spectrum. Parameter values are 'obust (cf. Table 1) and can be modified for)ther oceanic regimes. Although developed 'or the coastal waters of the San Juan Islands, the model will be further developed 'or environments with different species, pigment compositions, package effects, and increased pheophytin-to-chlorophyll ratios.

For this model to be successful in oligotrophic waters where cells are smaller and ıutrients may be limiting, methods are ıeeded to culture cyanobacteria and tiny)rochlorophytes under representative light ınd nutrient conditions to develop appro)riate values of $\phi_{436:676}$ for subtropical waters. Additionally, a method to remove :he pheopigment absorption from the methanol-extracted pigments, which includes)ackaging effects, is needed to test this and similar models in regions with large pheophytin-to-chlorophyll ratios.

This model lays the basis for partitioning photon absorption from direct in situ measurements of total absorption, which should be available in the near future (cf. Zaneveld et al. 1988). The potential for partitioning photons absorbed in a water volume into those absorbed by photosynthetic and non-photosynthetic absorbers has been explored and appears feasible. Diverse environments need to be individually assessed to modify the model developed here to specific optical domains. For environments in and near Puget Sound, even when absorption by gelbstoff and detritus dominated the total component absorption, errors for modeled absorption by in vivo phytoplankton were only ±15%.

References

BANNISTER, T. T. 1974. Production equations in terms of chlorophyll concentration, quantum yield, and upper limit to production. Limnol. Oceanogr. **19:** 1–12.

———, AND A. D. WEIDEMANN. 1984. The maximum quantum yield of phytoplankton photosynthesis in situ. J. Plankton Res. **6:** 275–294.

BIDIGARE, R. R., J. H. MORROW, AND D. A. KIEFER. 1989. Derivation analysis of spectral absorption by photosynthetic pigments in the western Sargasso Sea. J. Mar. Res. **47:** 323–341.

BRICAUD, A., A.-L. BÉDHOMME, AND A. MOREL. 1988. Optical properties of diverse phytoplanktonic species: Experimental results and theoretical interpretation. J. Plankton Res. **10:** 851–873.

———, A. MOREL, AND L. PRIEUR. 1981. Absorption by dissolved organic matter of the sea (yellow substance) in the UV and visible domains. Limnol. Oceanogr. **26:** 43–53.

CARDER, K. L., AND OTHERS. 1986. The interaction of light with phytoplankton in the marine environment, p. 42–55. *In* Ocean Optics 8, Proc. SPIE **637.**

———, AND R. G. STEWARD. 1985. A remote-sensing reflectance model of a red-tide dinoflagellate off west Florida. Limnol. Oceanogr. **30:** 286–298.

———, ———, G. R. HARVEY, AND P. B. ORTNER. 1989. Marine humic and fulvic acids: Their effects on remote sensing of ocean chlorophyll. Limnol. Oceanogr. **34:** 68–81.

CARPENTER, E. J., AND J. S. LIVELY. 1980. Review of the estimates of algal growth using ^{14}C tracer techniques, p. 161–178. *In* Primary productivity in the sea. Brookhaven Symp. Biol. 31. Plenum.

DAVIES-COLLEY, R. J., AND W. N. VANT. 1987. Absorption of light by yellow substance in freshwater lakes. Limnol. Oceanogr. **32:** 415–425.

GOLDMAN, J. C. 1988. Spatial and temporal discontinuities of biological processes in pelagic surface waters, p. 273–296. *In* B. J. Rothschild [ed.], Towards a theory on biological and physical processes in the world ocean. Reidal.

HENDRY, G. A. F., J. D. HOUGHTON, AND S. B. BROWN. 1987. The degradation of chlorophyll—a biological enigma. New Phytol. **107:** 255–302.

HØJERSLEV, N. K. 1980. On the origin of yellow substance in the marine environment, p. 39–56. *In* Studies in physical oceanography. Univ. Copenhagen, Inst. Phys. Oceanogr. Rep. 42.

ITURRIAGA, R., B. G. MITCHELL, AND D. A. KIEFER. 1988. Microphotometric analysis of individual particle absorption spectra. Limnol. Oceanogr. **33:** 128–135.

———, AND D. A. SIEGEL. 1988. Discrimination of the absorption properties of marine particulates using a microphotometric technique, p. 277–287. *In* Ocean Optics 9, Proc. SPIE **925**.

JASSBY, A. D., AND T. PLATT. 1976. Mathematical formulation of the relationship between photosynthesis and light for phytoplankton. Limnol. Oceanogr. **21:** 540–547.

JERLOV, N. G. 1968. Optical oceanography. Elsevier.

KALLE, K. 1966. The problem of the gelbstoff in the sea. Oceanogr. Mar. Biol. Annu. Rev. **4:** 91–104.

KIEFER, D. A., AND J. B. SOOHOO. 1982. Spectral absorption by marine particles of coastal waters of Baja California. Limnol. Oceanogr. **27:** 492–499.

KIRK, J. T. O. 1976. Yellow substance (gelbstoff) and its contribution to the attenuation of photosynthetically active radiation in some inland and coastal southeastern Australian waters. Aust. J. Mar. Freshwater Res. **27:** 61–71.

———. 1983. Light and photosynthesis in aquatic environments. Cambridge.

KISHINO, M., C. R. BOOTH, AND N. OKAMI. 1984. Underwater radiant energy absorbed by phytoplankton, detritus, dissolved organic matter, and pure water. Limnol. Occanogr. **29:** 340–349.

———, N. OKAMI, M. TAKAHASHI, AND S. ICHIMURA. 1986. Light utilization efficiency and quantum yield of phytoplankton in a thermally stratified sea. Limnol. Oceanogr. **31:** 557–566.

———, M. TAKAHASHI, N. OKAMI, AND S. ICHIMURA. 1985. Estimation of the spectral absorption coefficients of phytoplankton in the sea. Bull. Mar. Sci. **37:** 634–642.

KOPELEVICH, O. V., AND V. I. BURENKOV. 1977. Relation between the spectral values of the light absorption coefficients of sea water, phytoplankton pigments, and the yellow substance. Oceanology **17:** 278–282.

LORENZEN, C. J., AND S. W. JEFFREY. 1980. Determination of chlorophyll in seawater. UNESCO Tech. Pap. Mar. Sci. V. 35.

LUNDGREN, B. 1976. Spectral transmittance measurements of the Baltic. Univ. Copenhagen, Inst. Phys. Oceanogr. Rep. 30.

MASKE, H., AND H. HAARDT. 1987. Quantitative in vivo absorption spectra of phytoplankton: Detrital absorption and comparison with fluorescence excitation spectra. Limnol. Oceanogr. **32:** 620–633.

MITCHELL, B. G., AND D. A. KIEFER. 1984. Determination of absorption and fluorescence excitation spectra for phytoplankton, p. 157–169. *In* O. Holm-Hansen et al. [eds.], Marine phytoplankton and productivity. Springer.

———, AND ———. 1988. Clorophyll *a* specific absorption and fluorescence excitation spectra for light-limited phytoplankton. Deep-Sea Res. **35:** 639–663.

MOREL, A. 1974. Optical properties of pure seawater, p. 1–24. *In* N. G. Jerlov and E. Steemann Nielsen [eds.], Optical aspects of oceanography. Academic.

———, AND A. BRICAUD. 1981. Theoretical results concerning light absorption in a discrete medium, and applications to specific absorption of phytoplankton. Deep-Sea Res. **28:** 1375–1393.

———, AND L. PRIEUR. 1975. Analyse spectrale des coefficients d'atténuation diffuse, de réflexion diffus, d'absorption et de rétrodiffusion pour diverses régions marines. Centre Rech. Oceanogr. Villefranche-sur-Mer Rapp. 17. 157 p.

———, AND ———. 1976. Irradiation journalière en surface et mesure des éclairements sous marins; flux de photons et analyse spectrale, p. 1–256. *In* Résultats de la campagne CINECA 5 (Groupe Mediprod), Sect. 1.1–10. Publ. CNEXO.

MORROW, J. H., W. S. CHAMBERLIN, AND D. A. KIEFER. 1989. A two-component description of spectral absorption by marine particles. Limnol. Oceanogr. **34:** 1500–1509.

OKAMI, N., M. KISHINO, S. SUGIHARA, N. TAKEMATSU, AND S. UNOKI. 1982. Analysis of ocean color spectra. 3. Measurements of optical properties of sea water. J. Oceanogr. Soc. Jpn. **38:** 362–372.

PERRY, M. J., AND S. M. PORTER. 1989. Determination of the cross-section absorption coefficient of individual phytoplankton cells by analytical flow cytometry. Limnol. Oceanogr. **34:** 1727–1738.

PETERSON, B. J. 1980. Aquatic primary productivity and the ^{14}C-CO_2 method: A history of the productivity problem. Annu. Rev. Ecol. Syst. **11:** 359–385.

PLATT, T., AND A. D. JASSBY. 1976. The relationship between photosynthesis and light for natural assemblages of coastal marine phytoplankton. J. Phycol. **12:** 421–430.

PRIEUR, L., AND S. SATHYENDRANATH. 1981. An optical classification of coastal and oceanic waters based on the specific spectral absorption curves of phytoplankton pigments, dissolved organic matter, and other particulate materials. Limnol. Oceanogr. **26:** 671–689.

SATHYENDRANATH, S., L. LAZZARA, AND L. PRIEUR. 1987. Variations in the spectral values of specific absorption of phytoplankton. Limnol. Oceanogr. **32:** 403–415.

SMITH, R. C., AND K. S. BAKER. 1981. Optical properties of the clearest natural waters. Appl. Opt. **20:** 177–184.

TREES, C. C., AND K. J. VOSS. 1988. Absorption measurements of phytoplankton using optoacoustic spectroscopy. Eos **69:** 1109.

VERNET, M., AND C. J. LORENZEN. 1987. The relative abundance of pheophorbide *a* and pheophytin *a* in temperate marine waters. Limnol. Oceanogr. **32:** 352–358.

YENTSCH, C. S. 1962. Measurement of visible light absorption by particulate matter in the ocean. Limnol. Oceanogr. **7:** 207–217.

ZANEVELD, J. R. V., R. BARTZ, J. C. KITCHEN, AND R. W. SPINRAD. 1988. A reflective-tube diffuse attenuation meter and absorption meter. Eos **69:** 1125.